

Insights into the great M_w 7.9 Nepal earthquake of 25 April 2015

Prosanta Kumar Khan^{1,*}, Md. Afroz Ansari² and Dhananjay Singh¹

¹Department of Applied Geophysics, Indian Institute of Technology (Indian School of Mines), Dhanbad 826 007, India

²Life, Environmental and Earth Sciences Division, University of Bucharest, Romania

The 2015 M_w 7.9 earthquake occurred in the Nepal Himalaya between the Indian and Asian plates. The gravity modelling has been carried out along a 2D trench-orthogonal profile passing through the epicentre of this earthquake. The projections of mainshocks and aftershocks show their major confinement around the bending segment of the Indian upper crust (IUC). The operative shallowly plunging maximum compressive stress led to the accumulation of strain energy around the bending zone of the IUC, and triggered thrust-dominated southward movement of the Indian crustal block along a shallowly, dipping shear plane in the anisotropic layer. This can be broadly explained by three-stage rupture processes: the first one was associated with slow nucleation and rupture growth for early ~ 15 sec, the second one migrated upward, rupturing the uppermost part of the IUC for the next ~ 10 sec, and the third one propagated very fast during deformation for the remaining ~ 25 sec till the fracture-tip reached the overlying brittle Asian crust.

Keywords: 2015 Nepal earthquake, frictional sliding, gravity modelling, Indian upper crust.

THE present study aims at understanding the tectonogenesis behind the occurrences of two recent great earthquakes of magnitude (M_w) 7.9 and 7.2 during April–May 2015 beneath the Nepal Himalaya. Segment-specific seismic activities^{1,2}, rotational underthrusting and concomitant uneven southward migration of the Asian crust^{3,4}, along-strike wide variation of the Indian plate obliquity (Figure 1), and occurrence of seismicity in the mantle–lithosphere of the Indian plate⁵ clearly account for lateral changes in the dynamics/kinematics of the Himalaya. Although several studies involving gravity modelling were carried out for Nepal–Sikkim Himalaya^{6–13}, the present study analyses the Bouguer gravity anomaly along a strike-orthogonal profile passing through the epicentre of the 7.9 magnitude Nepal earthquake for a detailed understanding of the spatial distribution of its aftershocks and other great shocks in this part of the Himalaya (Figure 2). The geometries of different layers in the descending Indian plate and the southward converging Asian crust (Figure 1) were initialized by other stud-

ies for minimizing the non-uniqueness in the modelling using Bouguer gravity anomaly data along the profile. Depth distributions of the Nepal mainshocks and aftershocks have been inspected in the reconstructed Indian lithosphere through gravity modelling. One major shock of magnitude (M_w) 5.0 that occurred in December 2014 has also been considered in the present analysis.

Tectonic framework

The Himalayan range was evolved through continued convergence of the Indian plate against the Asian plate since about 50 Ma (refs 14–19). The southward migration of thrust packages along the crustal-scale Main Central Thrust (MCT), Main Boundary Thrust (MBT) and Main Frontal Thrust (MFT) framed this diffused boundary into the present form of the Himalaya²⁰. The most recently activated thrust plane, MFT, particularly accommodates the deformation of the southward migrating landmass²¹. The MCT, MBT and MFT invariably terminate at northerly dipping basal detachment (i.e. decollement, figure 2 *d* of Schulte-Pelkum *et al.*²²) named the Main Himalayan Thrust (MHT). The Indian continental plate penetrates along the base of this thrust plate (i.e. MHT) towards the north below the Himalaya and southern Tibet^{5,23–31}.

Convergence of the Indian plate varies significantly between ~ 4.2 and 5.4 cm/yr (refs 32–34). This has caused the loading of the upper and middle layers, and further created compression and resulted in the flexure of the leading portion of the penetrating lithosphere, which subsequently allowed thickening of the Asian crust towards the northern part of the Himalaya⁷. The lithospheric strength partially supports the weight of the elevated mountains, and distributes the flexing load down near the front to evolve a basin³⁵. An increase in gravity gradient from the Indo-Gangetic Plain (~ 1 mGal/km) to the Greater Himalaya (GH) (2 mGal/km) accounts for more steepening of the Moho (i.e. $\sim 2^\circ$ – 3° to $\sim 10^\circ$ – 15°) from the Lesser to Greater Himalaya¹. Elevated topography like mountain belts normally exerts a force upon the adjacent plates³⁶. The force exerted on the neighbouring lowlands can be computed based on the elevation of topography and contrast in the crustal thickness³⁷. Seismic experiments show that the thickness of the crust increases to 70–80 km towards the north near southern

*For correspondence. (e-mail: kxanprosanta1966@gmail.com)

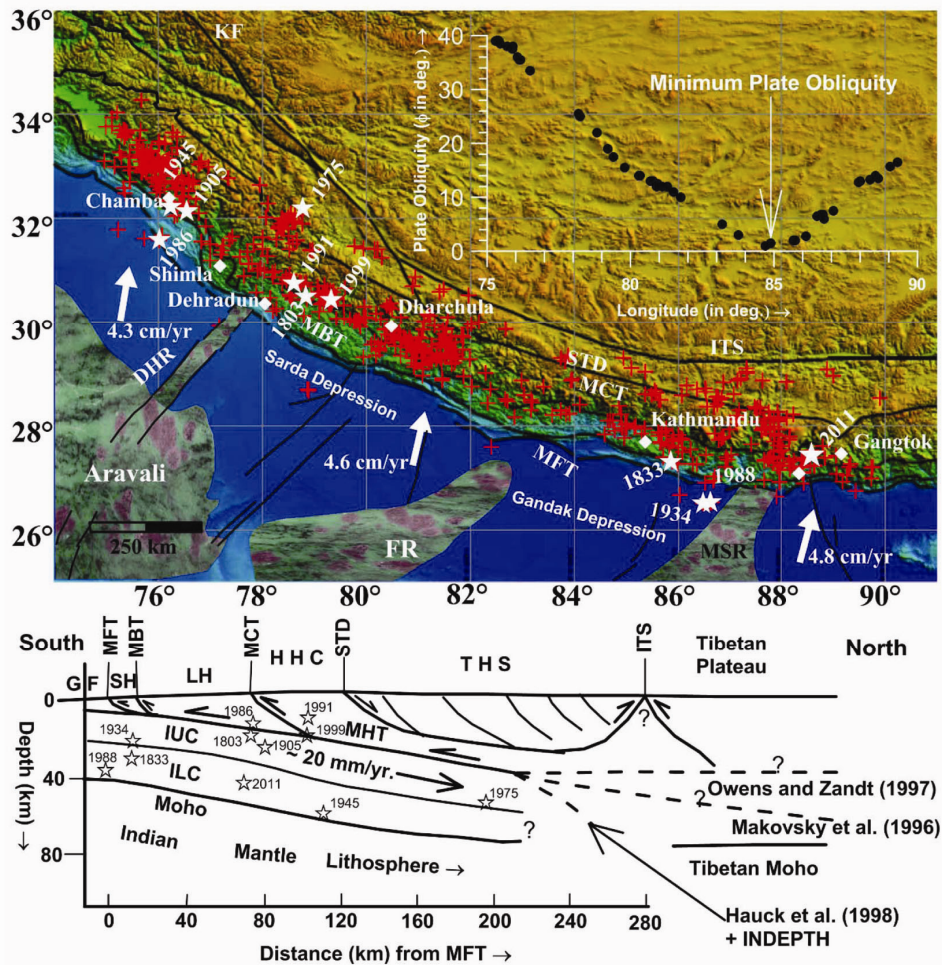


Figure 1. (Top) Map showing the distribution of 611 moderate magnitude earthquakes (+) and 11 historical damaging earthquakes (solid white stars) along the Central Himalaya. Solid arrows illustrate the Indian plate velocity vector with respect to the Asian plate (after DeMets *et al.*³²). (Bottom) Penetration of different crustal layers as well as the Indian mantle lithosphere below the Himalaya. Open stars represent the hypocentres of 11 historical earthquakes. MFT, Main Frontal Thrust; MCT, Main Central Thrust; MHT, Main Himalayan Thrust; STD, South Tibetan Detachment; ITS, Indus-Tsangpo Suture; GF, Gangetic Foreland; SH, Siwalik Himalaya; LH, Lesser Himalaya; GHC, Greater Himalayan Crystallines; THS, Tethys Himalaya Sediment; IUC, Indian Upper Crust; ILC, Indian Lower Crust; KF, Karakoram Fault; DHR, Delhi–Hardwar Ridge; FR, Faizabad Ridge; MSR, Monghyr–Saharsa Ridge.

Tibet^{25,38}, and the Tibetan Plateau exerts a large force against the Indian plate^{19,38}. This complies with the isostatic adjustment of this elevated landmass^{7–11,19,39,40}.

Study of seismicity and source mechanisms

Figure 1 shows the occurrences of 611 earthquake events ($M_w \geq 4.0$) during 1902–2012 in the central Himalayan arcuate belt². The epicentral parameters of these 611 events were compiled from the catalogue of the Indian Society of Earthquake Technology (ISET)⁴¹, International Seismological Centre (ISC) and US Geological Survey (USGS). Initially, 1755 earthquake events were compiled from the catalogues of ISC and USGS for the period from 1964 to 2012, and 81 events for the period from 1902 to 1963 from the catalogue of ISET for a region extending

from 26°N to 34.5°N and 75°E to 90°E. These 1836 events were scrutinized with reference to the central part of the Himalaya (Figure 1) and the magnitude restricted to 4.0 and above. The entire process has reduced the number of events to 611, and only three events with magnitude 6.5, 6.0 and 5.7 that occurred in 1945, 1947 and 1961 prior to 1964 were included in the final list for preliminary interpretation. Epicentres of these 611 events are plotted on the map (Figure 1) for a basic preliminary understanding of the relative concentration of seismicity in different parts of the Central Himalaya. Epicentres of historical damaging earthquakes predominantly concentrated in the area of clustered seismicity (Figure 1). An earlier study² reported that the seismic activities are apparently confined in some specific segments along the arc as noted in Figure 1. Depth-section study indicates

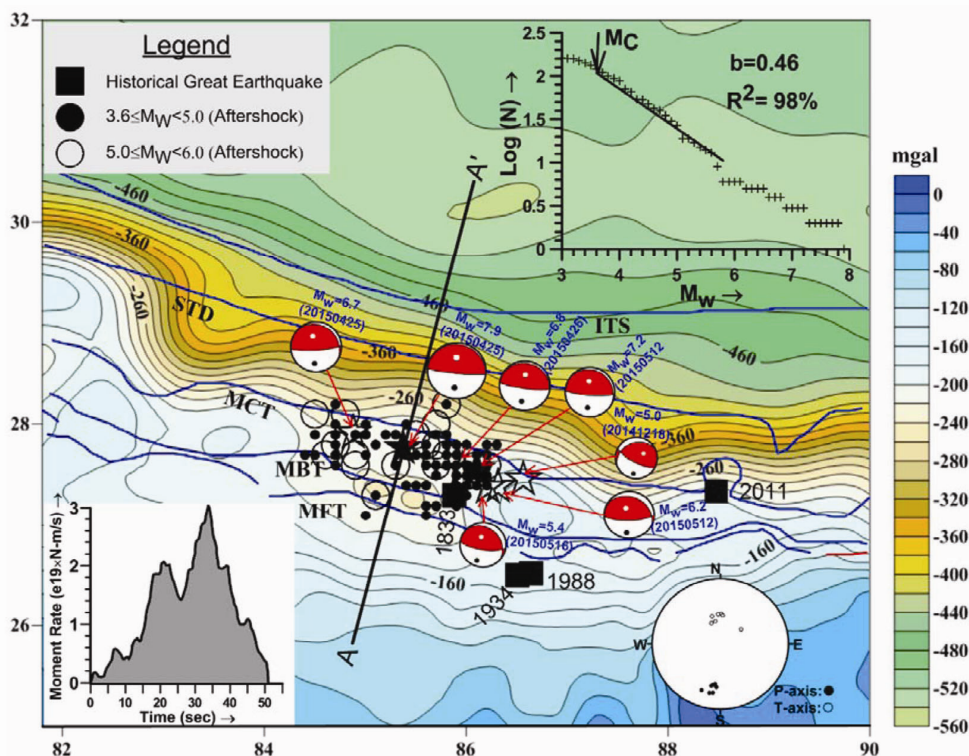


Figure 2. Contour lines plotted on the map indicating the variations of Bouguer gravity anomaly in the Nepal Himalaya (after EGM2008 gravity model). Profiles AA', passing through the epicentre of the M_w 7.9 Nepal earthquake of 25 April 2015 and normal to the strike of the Himalaya, were selected for gravity modelling. Beach balls illustrate the source mechanisms of the mainshocks and major aftershocks with magnitude and date are explained adjacent to them. Solid and open dots in the beach balls represent the maximum (P) and minimum (T) compressive stress axes. (Top right) Plot illustrating the computation of seismic b -value. M_c is the completeness magnitude. (Right bottom) Circle illustrating the stereographic projections of P and T axes. (Left bottom) Plot showing the moment energy release characteristics during the M_w 7.9 Nepal earthquake⁶⁹.

that earthquake sources are found to lie mainly between MBT and South Tibetan Detachment (STD), and are not associated with MHT. Khan *et al.*² concentrated seismic activities were mainly associated with the sharp flexing portions of the Indian upper crust (IUC), Indian lower crust (ILC) or uppermost mantle part of the northerly dipping Indian plate.

A total of 162 events, including 159 aftershocks, M_w 7.9 on 25 April 2015 and M_w 7.2 on 12 May 2015 mainshocks and one event (M_w 5.0) occurring on 18 December 2014 in Nepal area have been compiled. Of these 159 aftershocks, 114 events of m_b 3.6 and more have been used in the current analysis (Figure 2). Location parameters of these events, except the focal depth of M_w 7.9 mainshock, were collected from the USGS catalogue. These earthquake data motivated us to understand the tectonogenesis behind the occurrences of the two great earthquakes. The 2015 M_w 7.9 mainshock source zone (focal depth: 15 km, Avouac *et al.*⁴²; 16 km, Grandin *et al.*⁴³; 17.5–21 km, He *et al.*⁴⁴) accompanied maximum dislocation of 15–17.6 km (ref. 45) and tapering of slip at 15–20 km depth^{46,47} between MBT and MCT. These widely varying results allowed us to choose a depth of ~16 km of the 2015 M_w 7.9 mainshock. The aftershocks were found to be reasonably clustered in the area surrounding the

epicentre of the 25 April mainshock. The other mainshock of 12 May likely happened at the eastern boundary of the area of aftershock distributions. The epicentres of both these events were also near those of the 1833, 1934 and 1988 great damaging earthquakes (Figures 1 and 2).

Focal mechanisms of seven earthquakes having $M_w \geq 5.0$ (Figure 2) were taken from the Harvard CMT Catalogue. Mechanisms show that tectonic processes were dominated by thrust movements on approximately northward-directed dipping planes with inclination of not more than 24°. One event, apparently a foreshock, occurred on 18 December 2014 on a 26° dipping thrust plane along the N–S direction. Small strike–slip motions associated with few aftershocks, located at the eastern end of the event distributions, might indicate an eastward shift of the accumulated stress after the incidence of the 25 April mainshock. It is also clear from focal mechanisms that the maximum compressive stress axes (P) are dipping shallowly and directed along ~SSW–NNE and account for convergence of the Indian plate against the Asian landmass. It may be noted from Figure 2 that past the area of seismicity distribution towards north, the Bouguer gravity anomaly sharply decreases, which can only be resolved through visualization of the hypocentre distributions of the events. Further, a 2D gravity

modelling has been carried out to find their association with different layers in the descending Indian lithosphere.

Gravity modelling

Bouguer gravity anomaly data were compiled from EGM2008 gravity model. The gravity map was reconstructed following the exercise of Bouguer correction and terrain corrections. Although the Bouguer anomaly data were consistent with terrestrial data, the high frequency content of the signal was filtered out. Two-dimensional modelling was carried out along a profile perpendicular to the strike of the Himalaya, passing through the MFT, MBT, MCT, STD, etc. The initial layer parameters were considered after some studies in the literature^{5,22,27,48–50}. The initial densities of 2.30 g/cc (ref. 51), 2.45 g/cc, 2.67 g/cc (ref. 9) and 2.75 g/cc (ref. 52) were considered for the sediment near the IGP, Siwalik Himalayan Sediment (SHS), Lesser Himalayan Sediment (LHS) and GH respectively (Table 1). Different rheologies such as diabase (2.90 g/cc) for the southern Indian lower crust (SILC) and olivine (3.27 g/cc) for the upper mantle were used for the modelling⁹. In addition, the initial densities of 2.65 g/cc, 2.87 g/cc (ref. 11), 2.65 g/cc (ref. 12), 2.74 g/cc (ref. 53) and 2.98 g/cc (ref. 13) have been considered for the Tethys Himalayan Sediment (THS), Asian crust (AC), Granitic batholith (GB), northern Indian upper crust (NIUC) and northern Indian lower crust (NILC) respectively. A single fault geometry system is considered, where MCT, MBT and MFT merge with the MHT in the deeper part^{24,27,29}. With the adopted layer parameters, a preliminary model was reconstructed using Geosoft Oasis Montaj 8.4. Subsequently, densities and geometries of different geological units were modified through various steps of the iteration process. At each iteration, the fit between the observed and calculated responses was estimated and rms error reduced to 3.844 for the final model (Figure 3).

Table 1. Density of different geological units for the initial and final model

Crustal layers/ geological units	Initial density		Final density (g/cc)
	(g/cc)	Reference	
Indo-Gangetic Plain	2.30	51	2.28
Siwalik Himalaya Sediment	2.45	9	2.36
Lesser Himalaya Sediment	2.67	9	2.63
Greater Himalaya	2.75	52	2.75
Tethys Himalayan Sediment	2.65	11	2.65
Granitic Batholith	2.65	12	2.65
Asian crust	2.87	11	2.76
Southern Indian upper crust	2.67	9	2.71
Southern Indian lower crust	2.90	9	2.93
Northern Indian upper crust	2.74	53	2.80
Northern Indian lower crust	2.98	13	2.98
Indian Mantle Lithosphere	3.27	9	3.27

The gravity modelling indicates that the Conrad, between IUC and ILC, Moho and MHT are dipping shallowly below the IGP, Siwalik and Lesser Himalaya, in agreement with the observations of Nábělek *et al.*⁵ and Schulte-Pelkum *et al.*²². The dips of these crustal boundaries sharply increase towards the north beyond the Lesser Himalaya. The increasing gradients of the dips of different crustal layers beneath the GH reduce significantly past the TH towards southern Tibet. The Moho with average depth of 42 km near the IGP increases rapidly towards the north and reaches ~74 km beneath southern Tibet, documenting a locus bending with simultaneous loading of the Asian crust beneath the GH. Similarly, the ~25 km average depth of boundary between IUC and ILC beneath the Siwalik Himalaya (SH) sharply increases towards the north, and reaches ~50 km past GH. Change in depth of upper surface of the IUC is also quite sharp from SH (~11 km) to GH (~21 km).

Discussion and conclusions

The distribution of seismicity is critically examined below the different tectonic provinces of the Himalaya. Distinctive variation of seismicity distribution is apparently identified in different tectonic domains both from south to north and shallow to deeper levels in the converging Indian and Asian lithospheric plates. The region adjacent to the Lesser Himalaya (LH) recorded maximum concentration of seismic events (Figures 2 and 3). Further, most of the aftershocks, including the two mainshocks were confined within the IUC, and associated with the flexing segment of the converging Indian plate. Further, the ~12° average dip of the crustal layers between LH and GH reasonably complied with the ~11° average dip of the rupture planes of major shocks ($M_w > 6.5$). The hypocentres of the great 1833, 1934 and 1988 historical earthquakes were apparently located within the ILC and near its upper boundary (Figure 3). Although the great earthquakes were interpreted to be associated with the MHT^{42,54,55}, the role of the flexing segment of the converging Indian plate behind the occurrence of two recent great Nepal earthquakes cannot be ruled out. The occurrence of the great earthquakes in the zones of depressions towards the Himalayan foothills (Figure 1) might account for segment-specific distribution of earthquake events². The intersecting basement ridges to the foothills of the Himalaya apparently inhibit the occurrence of great earthquakes. Similar inferences were also drawn elsewhere along subduction margins^{56–58}. The bending portion of the lithosphere was probably the high-strained zone of stress accumulation⁵⁹, and deformed severely before the mainshock. The lower seismic *b*-value (estimated using earthquake magnitude–frequency empirical relation^{60–62}) and minimum Indian plate obliquity (~0°) support the accumulation of high compressional strain

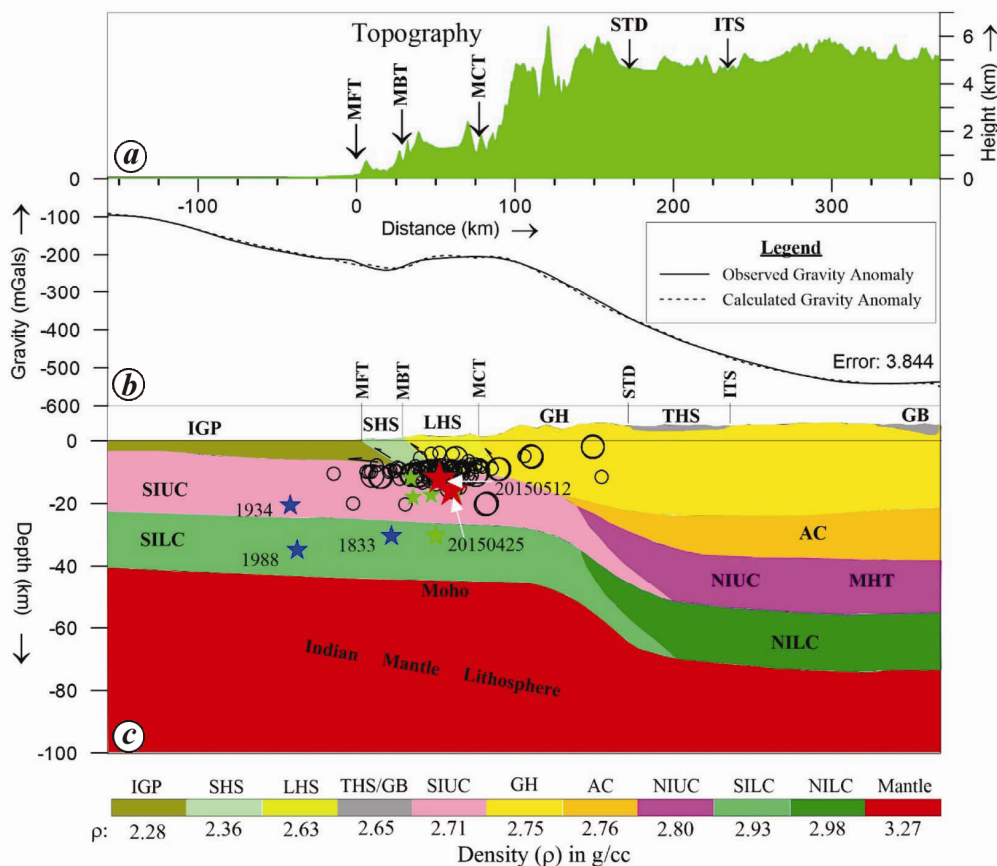


Figure 3. Plot showing 2D gravity modelling along profile AA'. *a*, Variation in the height of the Himalaya along AA' (after GTOPO 30). *b*, Comparison between observed and computed Bouguer gravity anomalies. *c*, 2D gravity–density model. Hypocentres of 114 aftershocks (open large and small circles), four large aftershocks and one foreshock (small green-coloured star), two mainshocks (large red-coloured stars), and the 1833, 1934 and 1988 damaging earthquakes (blue-coloured stars) are also shown. Magnitude ranges of events are explained in Figure 2. Other abbreviated terms are discussed in Figure 1 and Table 1.

energy in the ILC of the Indian plate, which was released through generation of two mainshocks and a number of aftershocks. The present results also corroborate the views of Pandey *et al.*⁶³.

Strain energy dissipation occurring through the flexing zone of the subducting lithosphere was estimated elsewhere to be about ~60% (ref. 64). The maximum strength of the oceanic lithosphere along plate margins was found to be an order of magnitude less than the maximum bending stress of the subducting lithosphere. Turcotte and Schubert⁶⁵ showed that ~90% of elastic strain energy is released through flexing segment of the subducting lithosphere in form of seismicity, and ~10% is used for its supporting with hardly any deformation. Intraplate origin of such great earthquakes along the subduction margin was also proposed elsewhere^{66–68}. The moment release characteristics during rupturing associated with the 25 April mainshock⁶⁹ clearly showed lower values for the initial ~15 sec, increasing gradually for the next ~10 sec, and later released drastically during remaining ~25 sec (Figure 2). The slow initiation of rupturing was possibly confined in the 6 km thick anisotropic fabric in the IUC

near the zone of locked to stable sliding^{22,30,31,70}. A three-stage fracture mechanism may be suggested for this rupture progression. An early nucleation process for ~15 sec (quasi-static crack growth) moved up with partial failure in the uppermost part of the IUC for the next ~10 sec, and finally, the fracture tip migration followed fast during deformation for a further ~25 sec till it reached to the overlying Asian crust⁷¹. In the present gravity model, the upper surface of the 6 km thick anisotropic layer appears to be dipping at a depth of ~7 km near the MFT to a depth of ~11 km near the MCT (Figure 3). Grandin *et al.*⁴³ identified a slow nucleation process of rupturing for the first 10 sec for this 2015 mainshock. Wang and Mori⁷², based on global dataset showed that the rupture slowly progressed with 1.0 km/sec speed for the first 20 sec, and later migrated with a higher speed of ~3.0 km/sec for the remaining 30–40 sec. These agree with the global observations that indicate a slow initiation and very fast expansion. The frictional sliding involving fracture along the fault contact in the upper brittle crust presumably caused the Himalaya to abruptly move southwestward towards the Indian plate by ~4.8 m (refs 73, 74).

1. Ni, J. and Barazangi, M., Seismotectonics of the Himalayan collision zone: geometry of the underthrusting Indian Plate beneath the Himalaya. *J. Geophys. Res.*, 1984, **89**, 1147–1163.
2. Khan, P. K., Ansari, M. A. and Mohanty, S., Earthquake source characteristics along the arcuate Himalayan belt: geodynamic implications. *J. Earth Syst. Sci.*, 2014, **123**, 1013–1030.
3. Klootwijk, C. T., Conaghan, P. J. and Powell, C. M., The Himalayan arc: large-scale continental subduction, oroclinal bending, and back-arc spreading. *Earth Planet. Sci. Lett.*, 1985, **75**, 316–319.
4. Willet, S. D. and Beaumont, C., Subduction of Asian lithospheric mantle beneath Tibet inferred from models of continental collision. *Nature*, 1994, **369**, 642–645.
5. Nábělek, J. *et al.*, Underplating in the Himalaya-Tibet Collision Zone revealed by the Hi-CLIMB Experiment. *Science*, 2009, **325**, 1371–1374.
6. Karner, G. D. and Watts, A. B., Gravity anomalies and flexure of the lithosphere at mountain ranges. *J. Geophys. Res.*, 1983, **88**(10), 449–477.
7. Lyon-Caen, H. and Molnar, P., Gravity anomalies, flexure of the Indian plate, and the structure, support and evolution of the Himalaya and Ganga Basin. *Tectonics*, 1985, **4**, 513–538.
8. Jin, Y., McNutt, M. K. and Zhu, Y. S., Mapping the descent of Indian and Eurasian plates beneath the Tibetan Plateau from gravity anomalies. *J. Geophys. Res.*, 1996, **101**, 11275–11290.
9. Cattin, R., Martelet, G., Henry, P., Avouac, J. P., Diament, M. and Shakya, T. R., Gravity anomalies, crustal structure and thermo-mechanical support of the Himalaya of Central Nepal. *Geophys. J. Int.*, 2001, **147**, 381–392.
10. Hetényi, G., Cattin, R., Vergne, J. and Nábělek, J. L., The effective elastic thickness of the India Plate from receiver function imaging, gravity anomalies and thermomechanical modeling. *Geophys. J. Int.*, 2006, **167**, 1106–1118.
11. Tiwari, V. M., Vyghreswara, R., Mishra, D. C. and Singh, B., Crustal structure across Sikkim, NE Himalaya from new gravity and magnetic data. *Earth Planet. Sci. Lett.*, 2006, **247**, 61–69.
12. Bai, B., Zhang, S. and Braitenberg, C., Crustal density structure from 3D gravity modeling beneath Himalaya and Lhasa blocks, Tibet. *J. Asian Earth Sci.*, 2013, **78**, 301–317.
13. Ansari, M. A. and Khan, P. K., Occurrences of damaging earthquakes between the Himachal and Darjeeling Himalayas: tectonic implications. *Acta Geophys.*, 2014, **62**, 699–736.
14. Patriat, P. and Achahe, J., India–Eurasia collision chronology has implications for crustal shortening and driving mechanism for plates. *Nature*, 1984, **311**, 615–621.
15. Gaetani, M. and Garzanti, E., Multicyclic history of the northern India continental margin (northwestern Himalaya). *Bull. Am. Assoc. Pet. Geol.*, 1991, **75**, 1427–1446.
16. de Sigoyer, J. *et al.*, Dating the Indian continental subduction and collisional thickening in the northwest Himalaya: multichronology of the Tso Moriri eclogites. *Geology*, 2000, **28**, 487–490.
17. Guillot, S., Garzanti, E., Baratoux, D., Marquer, D., Mahe' o, G. and de Sigoyer, J., Reconstructing the total shortening history of the NW Himalaya. *Geochem. Geophys. Geosyst.*, 2003, **4**(7), 1064.
18. Aikman, A. B., Harrison, T. M. and Lin, D., Evidence for Early (>44 Ma) Himalayan crustal thickening, Tethyan Himalaya, southeastern Tibet. *Earth Planet. Science Lett.*, 2008, **274**, 14–23.
19. Copley, A., Avouac, J. P. and Royer, J. Y., India–Asia collision and the Cenozoic slowdown of the Indian plate: implications for the forces driving plate motions. *J. Geophys. Res.*, 2010, **115**, B03410 (1–14).
20. Le Fort, P., Metamorphism and magmatism during the Himalayan collision. In *Collision Tectonics* (eds Coward, M. P. and Ries, A. C.), Geological Society of London, Special Publication, 1986, vol. 19, pp. 159–172.
21. Lavé, J. and Avouac, J. P., Active folding of fluvial terraces across the Siwaliks Hills, Himalayas of central Nepal. *J. Geophys. Res.*, 2000, **105**, 5735–5770.
22. Schulte-Pelkum, V., Monsalve, G., Sheehan, A., Pandey, M. R., Sapkota, S., Bilham, R. and Wu, F., Imaging the Indian subcontinent beneath the Himalaya. *Nature*, 2005, **435**, 1222–1225.
23. Srivastava, P. and Mitra, G., Thrust geometries and deep structure of the outer and lesser Himalaya, Kumaon and Garhwal (India): implications for evolution of the Himalayan fold-and-thrust belt. *Tectonics*, 1994, **13**, 89–109.
24. Makovsky, Y., Klemperer, S. L., Huang, L. and Project INDEPTH Team, Structural elements of the southern Tethyan Himalaya crust from wide-angle seismic data. *Tectonics*, 1996, **15**, 997–1005.
25. Nelson, K. D. *et al.*, Partially molten middle crust beneath southern Tibet: synthesis of project INDEPTH results. *Science*, 1996, **274**, 1684–1688.
26. DeCelles, P. G., Gehrels, G. E., Quade, J. and Ojha, T. P., Eocene–early Miocene foreland basin development and the history of Himalayan thrusting, western and central Nepal. *Tectonics*, 1998, **17**, 741–765.
27. Hauck, M. L., Nelson, K. D., Brown, L. D., Zhao, W. and Ross, A. R., Crustal structure of the Himalaya orogen at ~90° east longitude from INDEPTH deep reflection profiles. *Tectonics*, 1998, **17**, 481–500.
28. Mukul, M., The geometry and kinematics of the Main Boundary Thrust and related neotectonics in the Darjiling Himalayan fold-and-thrust belt, West Bengal, India. *J. Struct. Geol.*, 2000, **22**, 1261–1283.
29. Bollinger, L., Henry, P. and Avouac, J. P., Mountain building in the Nepal Himalaya: thermal and kinematic model. *Earth Planet. Sci. Lett.*, 2006, **244**, 58–71.
30. Mukul, M., Jaiswal, M. and Singhvi, A. K., Timing of recent out-of-sequence active deformation in the frontal Himalayan wedge: insights from the Darjiling sub-Himalaya, India. *Geology*, 2007, **35**, 999–1002.
31. Mukul, M., First-order kinematics of wedge-scale active Himalayan deformation: insights from Darjiling–Sikkim–Tibet (DaSiT) wedge. *J. Asian Earth Sci.*, 2010, **39**, 645–657.
32. DeMets, C., Gordon, R. G., Argus, D. F. and Stein, S., Effect of recent revisions to the geomagnetic reversal time scale and estimates of current plate motions. *Geophys. Res. Lett.*, 1994, **21**, 2191–2194.
33. Larson, K. M., Bürgmann, R., Bilham, R. and Freymuelle, J. T., Kinematics of the India–Eurasia collision zone from GPS measurements. *J. Geophys. Res.*, 1999, **104**, 1077–1093.
34. Bettinelli, P., Avouac, J.-P., Flouzat, M., Jouanne, F., Bollinger, L., Willis, P. and Chitrakar, G. R., Plate motion of India and interseismic strain in the Nepal Himalaya from GPS and DORIS measurements. *J. Geodesy*, 2006, **80**, 567–589.
35. Lyon-Caen, H. and Molnar, P., Constraints on the structure of the Himalaya from an analysis of gravity anomalies and a flexural model of the lithosphere. *J. Geophys. Res.*, 1983, **88**, 8171–8192.
36. Artyushkov, E. V., Stresses in the lithosphere caused by crustal thickness inhomogeneities. *J. Geophys. Res.*, 1973, **78**, 7675–7708.
37. Molnar, P. and Lyon-Caen, H., Some simple physical aspects of the support, structure, and evolution of mountain belts. *Geol. Soc. Am. Spec. Pap.*, 1988, **218**, 179–208.
38. Hirn, A., Jobert, G., Wittlinger, G., Zhong-Xin, X. and En-Yuan, G., Main features of the upper lithosphere in the unit between the High Himalayas and the Yarlung Angbo Jiang suture. *Ann. Geophys.*, 1984, **2**, 113–118.
39. McKenzie, D. and Fairhead, D., Estimates of effective elastic thickness of the continental lithosphere from Bouguer and gravity anomalies. *J. Geophys. Res.*, 1997, **102**, 27523–27552.
40. Watts, A. B. and Burov, E. B., Lithospheric strength and its relationship to the elastic and seismogenic layer thickness. *Earth Planet. Sci. Lett.*, 2003, **213**, 113–131.
41. Bapat, A., Kulkarni, R. C. and Guha, S. K., Catalogue of earthquakes in India and neighborhood – from historical period up to

RESEARCH ARTICLES

1979. Indian Society of Earthquake Technology, Roorkee, 1983, p. 211.
42. Avouac, J.-P., Meng, L., Wei, S., Wang, T. and Ampuero, J.-P., Unzipping lower edge of locked Main Himalayan thrust during the 2015, *Mw* 7.8 Gorkha earthquake. *Nature Geosci.*, 2015, **8**, 708–711.
43. Grandin, R., Vallée, M., Satriano, C., Lacassin, R., Klinger, Y., Simoes, M. and Bollinger, L., Rupture process of the *Mw* = 7.9 2015 Gorkha earthquake (Nepal): Insights into Himalayan megathrust segmentation. *Geophys. Res. Lett.*, 2015, **42**, 8373–8382.
44. He, X., Ni, S., Ye, L., Lay, T., Liu, Q. and Koper, K. D., Rapid seismological quantification of source parameters of the 25 April 2015 Nepal earthquake. *Seismol. Res. Lett.*, 2015, **86**, 1568–1577.
45. Wu, Y. *et al.*, Coseismic deformations of the 2015 *Mw* 7.8 Gorkha earthquake and interseismic strain accumulation in the Himalayan tectonic belt and Tibetan plateau. *Tectonophysics*, 2016, **670**, 144–154.
46. Galetzka, J. *et al.*, Slip pulse and resonance of the Kathmandu basin during the 2015 Gorkha earthquake, Nepal. *Science*, 2015, **349**, 1091–1095.
47. Zhang, G., Hetland, E. and Shan, X., Slip in the 2015 *Mw* 7.9 Gorkha and *Mw* 7.3 Kodari, Nepal, earthquakes revealed by seismic and geodetic data: delayed slip in the Gorkha and slip deficit between the two earthquakes. *Seismol. Res. Lett.*, 2015, **86**, 1578–1586.
48. DMG, Exploration opportunities in Nepal. Department of Mines and Geology, Kathmandu, 1990, p. 32.
49. Brown, L. D. *et al.*, Bright spots, structure, and magmatism in southern Tibet from INDEPTH seismic reflection profiling. *Science*, 1996, **274**, 1688–1690.
50. Lemonnier, C. *et al.*, Electrical structure of the Himalaya of Central Nepal: high conductivity around the mid-crustal ramp along the MHT. *Geophys. Res. Lett.*, 1999, **26**, 3261–3264.
51. Gansser, A., The geodynamic history of the Himalaya. In *Zagros, Hindu-Kush, Himalaya. Geodynamic Evolution* (eds Gupta, H. K. and Delany, F. M.), American Geophysical Union, Geodynamics Series 3, Washington, DC, USA, 1981, pp. 111–121.
52. Jimenez-Munt, I., Fernandez, M., Jaume, V. and John, P. P., Lithosphere structure underneath the Tibetan Plateau inferred from elevation, gravity and geoid anomalies. *Earth Planet. Sci. Lett.*, 2008, **267**, 276–289.
53. Hetényi, G., Cattin, R., Brunet, F., Bollinger, L., Vergne, J., Nábělek, J. L. and Diament, M., Density distribution of the India plate beneath the Tibetan plateau: Geophysical and petrological constraints on the kinetics of lower-crustal eclogitization. *Earth Planet. Sci. Lett.*, 2007, **264**, 226–244.
54. Hough, S. E., Introduction to the Focus Section on the 2015 Gorkha, Nepal, earthquake. *Seismol. Res. Lett.*, 2015, **86**, 1502–1505.
55. Hayes, G. P. *et al.*, Rapid characterization of the 2015 *Mw* 7.8 Gorkha, Nepal, earthquake sequence and its seismotectonic context. *Seismol. Res. Lett.*, 2015, **86**, 1557–1567.
56. Kelleher, J. and McCann, W., Buoyant zones, great earthquakes, and unstable boundaries of subduction. *J. Geophys. Res.*, 1976, **81**, 4885–4898.
57. McGeary, S., Nur, A. and Ben-Avraham, Z., Spatial gaps in arc volcanism: the effect of collision or subduction of oceanic plateaus. *Tectonophysics*, 1985, **119**, 195–221.
58. Gutscher, M.-A., Malavieille, J., Lallemand, S. and Collot, J.-Y., Tectonic segmentation of the North Andean margin: impact of the Carnegie Ridge collision. *Earth Planet. Sci. Lett.*, 1999, **168**, 255–270.
59. Khan, P. K. and Chakraborty, P. P., Two-phase opening of Andaman Sea: a new seismotectonic insight. *Earth Planet. Sci. Lett.*, 2005, **229**, 259–271.
60. Gutenberg, B. and Richter, C. F., *Seismicity of the Earth and Associated Phenomenon*, Princeton University Press, Princeton, NJ, USA, 1954.
61. Khan, P. K. and Chakraborty, P. P., The seismic *b* value and its correlation with Bouguer gravity anomaly over the Shillong plateau area: a new insight for tectonic implication. *J. Asian Earth Sci.*, 2007, **29**, 136–147.
62. Khan, P. K., Ghosh, M., Chakraborty, P. P. and Mukherjee, D., Seismic *b*-value and the assessment of ambient stress in Northeast India. *Pure Appl. Geophys.*, 2011, **168**, 1693–1706.
63. Pandey, M. R., Tandukar, R. P., Avouac, J. P., Vergne, J. and Héritier, Th., Seismotectonics of the Nepal Himalaya from a local seismic network. *J. Asian Earth Sci.*, 1999, **17**, 703–712.
64. Conrad, C. P. and Hager, B. H., Effects of plate bending and fault strength at subduction zones on plate dynamics. *J. Geophys. Res.*, 1999, **104**, 17551–17571.
65. Turcotte, D. L. and Schubert, G., *Geodynamics Applications of Continuum Physics to Geological Problems*, Wiley, New York, USA, 1982, p. 450.
66. Singh, S. C. *et al.*, Seismic evidence for broken oceanic crust in the 2004 Sumatra earthquake epicentral region. *Nature Geosci.*, 2008, **1**, 777–781.
67. Khan, P. K. and Chakraborty, P. P., Bearing of plate geometry and rheology on shallow-focus mega-thrust seismicity with special reference to 26 December 2004 Sumatra event. *J. Asian Earth Sci.*, 2009, **34**, 480–491.
68. Khan, P. K., Chakraborty, P. P., Tarafder, G. and Mohanty, S., Testing the intraplate origin of mega-earthquakes at subduction margins. *Geosci. Front.*, 2012, **3**, 473–481.
69. Satriano, C., Analysis fact sheet, 2015; <http://www.ipgp.fr/en/central-nepal-earthquake-april-25th-2015>
70. Bilham, R., Larson, K. and Freymüller, J., GPS measurements of present-day convergence across the Nepal Himalaya. *Nature*, 1997, **386**, 61–64.
71. Lyakhovskiy, V., Scaling of fracture length and distributed damage. *Geophys. J. Int.*, 2001, **144**, 114–122.
72. Wang, D. and Mori, J., Short-period energy of the 25 April 2015 *Mw* 7.8 Nepal earthquake determined from backprojection using four arrays in Europe, China, Japan, and Australia. *Bull. Seismol. Soc. Am.*, 2016, **106**, 259–266.
73. Mitra, S., Paul, H., Kumar, A., Singh, S. K., Dey, S. and Powali, D., The 25 April 2015 Nepal earthquake and its aftershocks. *Curr. Sci.*, 2015, **108**, 1938–1943.
74. Reber, J. E., Lavier, L. L. and Hayman, N. W., Experimental demonstration of a semi-brittle origin for crustal strain transients. *Nature Geosci.*, 2015, **8**, 712–715.

ACKNOWLEDGEMENTS. We thank the Director, Indian Institute of Technology (ISM), Dhanbad for encouragement. P.K.K. acknowledges the financial support of SERB, Department of Science and Technology, Government of India, New Delhi. We thank the anonymous reviewers and handling editor for critical comments and suggestions, that helped improve the manuscript.

Received 2 February 2016; revised accepted 10 June 2017

doi: 10.18520/cs/v113/i10/2014-2020